Analyst

DNA Nanotechnology for Nucleic Acid Analysis: Sensing of Nucleic Acids with DNA Junction-Probes

Journal:	*Analyst*
Manuscript ID	AN-ART-10-2023-001707.R1
Article Type:	Paper
Date Submitted by the Author:	15-Dec-2023

Complete List of Authors:	Foguel, Marcos; University of Central Florida, Chemistry Zamora, Victor; Universidad Nacional de Ingenieria Facultad de Ciencias Ojeda, Julio; University of Central Florida, Chemistry Reed, Mark; University of Central Florida, Chemistry Bennett, Alexander; University of Central Florida, Chemistry Calvo-Marzal, Percy; University of Central Florida, Chemistry Gerasimova, Yulia; University of Central Florida, Department of Chemistry Kolpashchikov, Dmitry; University of Central Florida, Chemistry Chumbimuni-Torres, Karin; University of Central Florida, Chemistry; UTSA,

ARTICLE

DNA Nanotechnology for Nucleic Acid Analysis: Sensing of Nucleic Acids with DNA Junction-Probes

Received 00th January 20xx,
Accepted 00th January 20xx

DOI: 10.1039/x0xx00000x

Marcos V. Foguel,[a] Victor Zamora,[b] Julio Ojeda,[a] Mark Reed,[a] Alexander Bennett,[a] Percy Calvo-Marzal,[a] Yulia V. Gerasimova,[a] Dmitry Kolpashchikov,*[a,c] and Karin Y. Chumbimuni-Torres*[a]

DNA nanotechnology deals with the design of non-naturally occurring DNA nanostructures that can be used in biotechnology, medicine, and diagnostics. In this study, we introduced a nucleic acid five-way junction (5WJ) structure for direct electrochemical analysis of full-length biological RNAs. To the best of our knowledge, this is the first report on the interrogation of such long nucleic acid sequences by hybridization probes attached to a solid support. A hairpin-shaped electrode-bound oligonucleotide hybridizes with three adaptor strands, one of which is labeled with methylene blue (MB). The four strands are combined into a 5WJ structure only in the presence of specific DNA or RNA analytes. Upon interrogation of a full-size 16S rRNA in the total RNA sample, the electrode-bound MB-labeled 5WJ association produces a higher signal-to-noise ratio than electrochemical nucleic acid biosensors of alternative design. This advantage was attributed to the favorable geometry on the 5WJ nanostructure formed on the electrode's surface. The 5WJ biosensor is a cost-efficient alternative to the traditional electrochemical biosensors for the analysis of nucleic acids due to the universal nature of both the electrode-bound and MB-labeled DNA components.

Introduction

The DNA nanotechnology deals with the manufacturing of pre-designed nanostructures made of DNA.[1-3] For example, DNA nanostructures have been proposed for the delivery of anti-cancer drugs,[4-6] which promises to advance anti-cancer therapy. DNA origami approach was proposed for genotyping single nucleotide polymorphisms in DNA using atomic force microscopy.[7] More recently, sensitive and selective detection of a target RNA sequence was achieved using a reconfigurable DNA origami template and circular dichroism signaling.[8] Another relevant development utilized a DNA tetrahedron structure for electrochemical detection of specific nucleic acid analytes.[9-11]

We have been taking advantages of nanostructures for nucleic acid analysis to improve selectivity and sensitivity of hybridization sensors for human disease diagnostics.[12] Additionally, the synthesis cost associated with DNA sequences have been decreasing year by year, making nucleic acid based technologies more cost-effective.[13] Electrochemical analysis of nucleic acids brings the benefit of portability and compatibility with modern electronic devices and, therefore, is considered to be promising for molecular diagnostics.[14-22] Due to the challenges associated with these technologies, such as maximizing the interaction between targets and probes, as well as achieving homogeneous distribution on the sensing surface,[23] various designs have been proposed.[13, 23] Traditional electrochemical probes are stem-loop folded oligonucleotides attached to a gold electrode and conjugated with Red/Ox markers (e.g. methylene blue - MB).[18, 24] Binding a complementary nucleic acid target changes the conformation of the probe to the elongated probe-target duplex, which separates the MB label from the electrode's surface, thus reducing the electrochemical signal (Scheme 1A).

We modified this ON→OFF signaling system to create the X biosensor with OFF→ON signaling mode by using the immobilize DNA crossover (X) structure introduced by DNA nanotechnology.[25, 26] In the X biosensor, the presence of a cognate target triggers association of two adaptor strands (m-strand-X and f-strand), one of which is tagged with the MB label, and a universal DNA hairpin (UDH) strand, into a four-way junction (4WJ) structure, as shown in Scheme 1B. Upon 4WJ structure formation, the Red/Ox marker came in proximity with the electrode's surface to turn on the electrochemical signal. In addition to the ON signal, the electrochemical X biosensor demonstrated the advantages of: (i) high selectivity at ambient temperatures, which cannot be achieved by hairpin probes,[25-28] (ii) ability to detect point mutations in highly structured nucleic acids;[29] (iii) possibility to analyze different nucleic acid sequences using the same electrode-attached oligonucleotide probe.[30] A disadvantage of the X biosensor is that the sequence of its most expensive oligonucleotide component – the MB-labeled strand – is target-dependent. We hypothesized that implementation of a fifth strand,

[a] Department of Chemistry. University of Central Florida, 4000 Central Florida Boulevard, Orlando, Fl 32816, United States
[b] Escuela Professional de Quimica, Facultad de Ciencias, Universidad Nacional Ingenieria, Av. Tupac 210, Lima, Peru.
[c] Burnett School of Biomedical Science, university of Central Florida, 4000 Central Florida Boulevard, Orlando, Fl 32816, United States.
† Footnotes relating to the title and/or authors should appear here.
Electronic Supplementary Information (ESI) available: [details of any supplementary information available should be included here]. See DOI: 10.1039/x0xx00000x

which bears the MB-label and is complementary to one of the two adaptor strands, would enable using the same labeled oligonucleotide for any arbitrary target, leading to the creation of the five strands X biosensor (5S-X), (Scheme 1C). Making the MB-modified strand independent of the target's sequence and, therefore, universal. This is important considering the high cost of such oligonucleotides. It keeps up with the strategy of universal biosensors, in which a single labeled probe can be utilized for the detection of potentially any nucleic acid sequence.[31]

Five-way DNA junction (5WJ) is a non-naturally occurring structure, first investigated by Wang in 1991[32] and Kadrmas in 1995.[33] In this study, we adopted the 5WJ structure for electrochemical detection of nucleic acids. In the 5WJ biosensor, the labeled MB-probe-5WJ is complementary to fragments of UDH and m-strand-5WJ, but not to the target (Scheme 1D). Initially, we were driven by the idea of using a universal MB-labeled probe. We accidentally discovered that the 5WJ electrochemical biosensor had unexpected advantages when used for the detection of a full-length biological RNA.

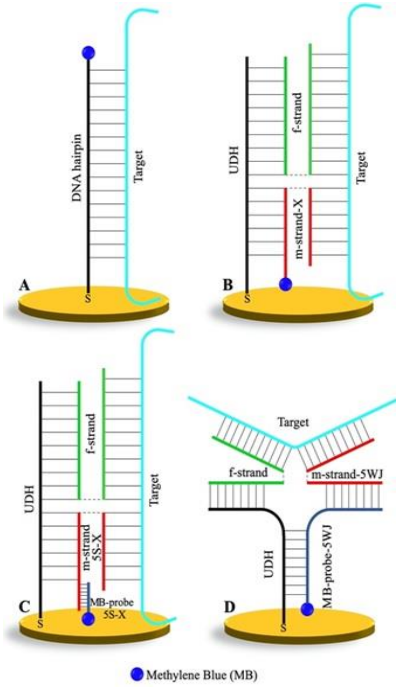

Scheme 1. Probe-target complexes formed in different designs of electrochemical nucleic acid biosensors: (A) a stem-loop probe labelled with MB in complex with a nucleic acid target; (B) X biosensor; (C) 5S-X biosensor; and (D) 5WJ biosensor. All the oligonucleotide sequences used in this work are shown in Table S1.

Material and Methods

All materials and chemicals used here are listed in the supplemental material.

Biosensors preparation

First, all the gold disk electrodes (GDEs) were cleaned by immersion in a piranha solution (1:3 ratio of 30% H2O2: 98% H_2SO_4 – CAUTION: piranha solution reacts violently with most organic materials and must be handled with extreme care) for 10 min. Then, the electrodes were rinsed with deionized water, manually polished with a microcloth and an alumina slurry (1.0 µm, 0.3 µm and 0.05 µm), and sonicated in deionized water and ethanol to remove residual alumina particles trapped on the electrode surface. Finally, the GDEs were activated in 0.5 M H_2SO_4 and via cyclic voltammetry (CV) from +1.6 to –0.1 V at a scan rate of 100 mV/s. The electrochemically active area of each GDE was determined through CV measurements.[34] The charge linked to the reduction peak of the oxygen monolayer from the surface of the gold electrode, along with the reference charge recommended for polycrystalline gold of 390 µC/cm^2,[35] was employed for area calculation. On average, the electrodes exhibited an electroactive area with a value of 0.033 ± 0.004 cm^2.

After the cleaning step, a universal DNA hairpin (UDH) was immobilized on the GDE. For this, initially, the disulfide bond of 1.0 µM UDH was reduced with 1.0 mM tris(2-carboxyethyl) phosphine hydrochloride (TCEP) by shaking the solution for 1 h at room temperature. Then, the solution was diluted with immobilization buffer (IB) to obtain a UDH final concentration of 0.1 µM, and drop-casted (15 µL) on the GDE with an incubation of 30 min. The electrodes were rinsed with IB, dried with nitrogen, and 15 µL of 2 mM 6-mercapto-1-hexanol (MCH) was drop-casted and incubated on the GDE for 30 min to prevent nonspecific adsorption. These monothiol bonds, when bonded to gold surfaces, have been shown to be stable for up to 15 days under buffer conditions.[36] The electrodes were rinsed with IB solution and dried with nitrogen.[26, 30, 37] Next, 50 µL of hybridization solution was prepared relied on the biosensor design analyzed. (i) X biosensor: 0.50 µM f-strand and 0.25 µM m-strand-X were mixed with the target in hybridization buffer (HB); (ii) 5S-X biosensor: 0.50 µM f-strand, 0.10 µM m-strand-5S-X and 0.25 µM MB probe-5S-X were mixed with the target in HB; (iii) 5WJ biosensor: the target 0.50 µM f-strand, 0.10 µM m-strand-5WJ and 0.25 µM MB probe-5WJ were mixed with the target in HB. Then, 15 µL of hybridization solution was drop-casted and incubated on the modified GDE for variable times as specified in each section. When a synthetic target DNA was used, the hybridization solutions were drop-casted on the modified GDE at room temperature. However, for transcript RNA targets and E. coli total RNA target, the hybridization solutions were heated at 90 ºC for 2 min before adding to the biosensor in order to unwind the target sequence. The biosensor response was expressed as the current density peak (jp) calculated as the current signal for a sample minus the current for the baseline.

Electrochemical Measurements

The electrochemical measurements were performed with a CHI1230C Electrochemical Workstation (CH Instruments, Austin, USA). The electrochemical cell consisted of a modified GDE, Ag/AgCl (1 M KCl) and platinum wire, which were used as working, reference and working electrodes, respectively. Square Wave Voltammetry (SWV) measurements were recorded in HB solution at a potential range from 0.0 to −0.5 V, frequency of 100 Hz, amplitude of 70 mV, and step potential of 3 mV at room temperature. Nitrogen was bubbled into the electrochemical cell to remove oxygen before the measurements were conducted. At least three working electrodes were used in each experiment to acquire statistically significant data.

Results and Discussion

We compared the performance of the 5WJ biosensor with that of the X and 5S-X biosensors targeting 16S rRNA, which is routinely used for both identifications of bacterial species[38] and diagnostics of human diseases.[39] The 5WJ-forming strands, f-strand and m-strand-5WJ, contained flexible triethylene glycol linkers, which were introduced to stabilize the 5WJ structure as it was earlier stabilized by unpaired nucleotide linkers.[33] Initial optimizations of the hybridization conditions was performed using short DNA targets corresponding to the interrogated *E. coli* 16S rRNA fragments from either a non-pathogenic K12 strain (K12-Target) or a verotoxinogenic strain O157:H7 (O157-Target)[40] (Table S1). Concentrations of the adaptor strands for the X biosensor were optimized as described earlier.[30] The assay conditions for the 5S-X and 5WJ biosensors are summarized in Tables S2 and S3, respectively.

The expected structure of the 5WJ complex in the presence of the K12-Target is shown in Scheme S1. Analysis of the structure by gel electrophoresis revealed formation of a low-mobility complex at approximately 100 bp, which can be assigned to the 5WJ structure, only when all components of the 5WJ were present (Figure S1).

The selectivity of the three biosensors targeting the fragment of K12 *E. coli* 16S rRNA was assessed by comparing the biosensors' response to the presence of the fully complementary non-pathogenic K12-target and two-base mismatched O157-target representing the pathogenic *E. coli* strain. All three biosensors demonstrated the capability to effectively discriminate between the respective targets (Figure 1A). However, the target-induced response of the 5WJ biosensor was reduced around 3-fold in comparison with the other two biosensors (5.8 ± 0.6 μA/cm^2 compared to 21 ± 2 μA/cm^2 or 17 ± 2 μA/cm^2 for the X or 5S-X biosensor, respectively). We hypothesized that this lower response might be related to the complexity of the 5WJ structure, which requires more time for its formation on the electrode's surface. Indeed, the electrochemical response of the X and 5S-X biosensors started to plateau within 120 min (Figure 1B). On the other hand, the 5WJ biosensor responded linearly over this time, thus confirming slower kinetics for the formation of the MB-labeled complex on the electrode's surface. Importantly, all three biosensors produce a signal above the background even after 15-min hybridization.

The dependence of the biosensors' response on the concentration of synthetic K12-target was analyzed in the range of 0-25 nM after 90-min hybridization step (Figure 1C). In all the designs saturation appears around 50nM of target. The X biosensor exhibited a linear response with a limit of detection (LOD) of 0.40nM and a sensitivity of 0.53 μA/cm^2 nM. For the 5S-X biosensor the LOD was 0.30 nM and sensitivity of 0.22 μA/cm^2 nM. The 5WJ biosensor had a LOD of 0.50 nM and a sensitivity of 0.12 μA/cm^2 nM. Similarly, to the X-biosensor,[26] the UDH-modified gold electrode could be regenerated after formation of the 5WJ structure by simply rinsing it with water. Thus, the biosensor was re-used up to four times after the original hybridization of the probe strands with over 92% recovery (Figure S2) upon rinsing the biosensor with deionized water for 1 min and performing another hybridization step.

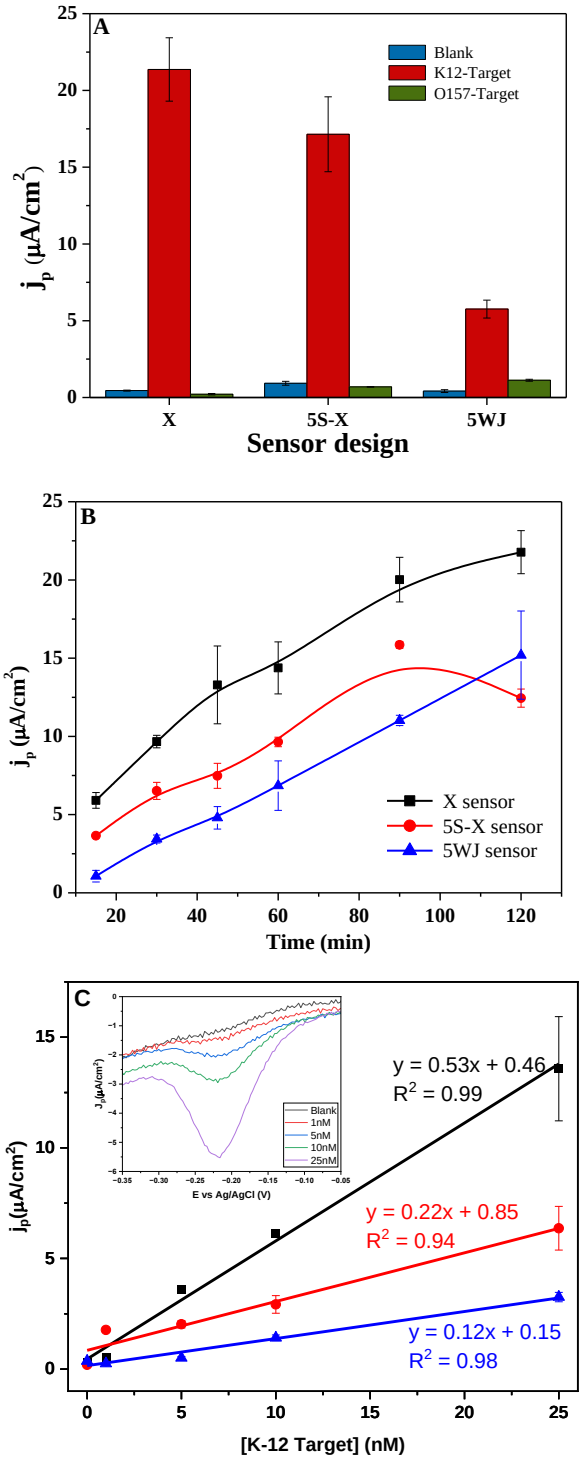

Figure 1. Electrochemical response of the 5WJ biosensor in comparison with the X and 5S-X biosensor. (A) Response of the biosensors in the absence of the target ("Blank", blue bars) and in the presence of either the fully matched K12-Target (red bars) or two based mismatched O157-Target (green bars) after 90-min hybridization on GDEs. (B) Hybridization time effect (15, 30, 45, 60, 90 and 120 min) in the presence of 50 nM K12-target. (C) Biosensor

calibration curves for K12-Target after 90-min hybridization. The data points for the X biosensor, 5S-X biosensor and 5WJ biosensor are depicted with black squares, red circles and blue triangles, respectively. Inset: SWV response of the 5WJ biosensor calibration curve between 0 and 25 nM.

After testing with DNA targets, the biosensors were evaluated using in vitro transcripts corresponding to full-length 16S rRNA (1541 nt) and 23S rRNA (2904 nt) from the nonpathogenic K12 *E. coli* strain. Figure 2A illustrates that all three biosensors generated a signal exceeding the background when exposed to their corresponding 16S rRNA targets. Notably, the signal produced by the 5WJ biosensor was 7 times higher than that of the other two biosensors. This discrepancy points to the superior efficacy of the 5WJ biosensor in detecting extended nucleic acid targets. This enhanced performance with longer sequences can be attributed to the positioning of the target within the 5WJ structure (Scheme 1), which situates it farther from the electrode's surface compared to the X or 5S-X biosensors. Therefore, the nucleotides of the target that extend beyond the double-stranded portions of the target-adaptor strand complexes do not disrupt the hybridization process of neighboring probes. This arrangement prevents any obstruction of the electrode, which could otherwise lead to a reduction in electron transfer.

Inspired by the discovered advantage of the 5WJ biosensor to interrogate long structured RNA, we tested whether the efficiency of the target recognition is retained if the target is in the mixture with other, non-specific, RNA. For this purpose, we used total RNA isolated from K12 *E. coli* cells. 16S rRNA constitutes ~30% of the total RNA preparation by mass,[41] with the rest comprised of other types of bacterial RNA including long 23S rRNA. The presence of competing RNA molecules affected the biosensor performance but could be mitigated by extending the hybridization time for the biosensor components to interact with the specific target and build the 5WJ associate on the surface of the electrode (compare responses of 5WJ E-biosensor shown in Figures 2B and S3). Indeed, upon a 3-h hybridization step, the total bacterial RNA sample containing about 50 nM 16S rRNA triggered a ~5-fold increase above the background (Figure S3). Remarkably, the 5WJ biosensor was the only one of the three E-biosensors studied that was able to detect 16S rRNA in the total bacterial RNA preparation (Figure 2B).

Additional attempts to establish a calibration curve using total RNA (depicted in Figure S4) demonstrated a comparable slope to the 5WJ biosensor calibrated with the K12 target (0.12 µAcm-2nm-1). The curve reached saturation at approximately 20nM of total RNA, with a corresponding LOD of 4.55nM. The observed saturation at low concentrations could be attributed to the long length of the RNA fragment.

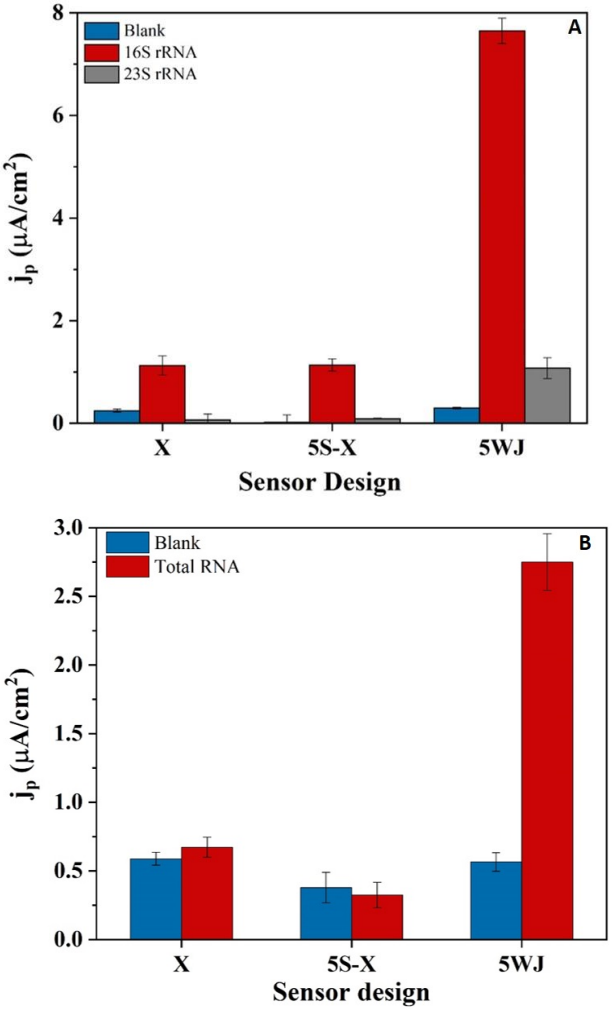

Figure 2. Response of the three biosensors in the absence of the targets ("Blank", blue bars); or in the presence of **A)** either 16S rRNA (red bars) or 23S rRNA transcripts (grey bars) at 50nM, after 90 minutes of hybridization time. **B)** K12 *E. coli* total RNA (red bars) after 3 hours of hybridization time. Total RNA concentration was 85.5 ng/µL, which corresponds to approximately 50 nM of 16S RNA. All hybridization solutions (containing RNA + adaptor strands + MB probe) were heated at 90 °C for 2 min before adding to the biosensor.

Electrochemical biosensors are well-known for their struggling with interrogation of long native nucleic acid sequences. For example, conventional hairpin probe biosensors (Scheme 1A) were unable to detect 16S rRNA even after thermal denaturation: RNA fragmentation was required to achieve signal above the background.[42, 43] In our earlier experiments, the signal in response to DNA targets of 141 nt was lower than that triggered by shorter targets (Figure S5). Likewise, the X and 5S-X biosensors demonstrated ~9- and 2.5-fold reduction in the signal intensity, respectively, when interrogated 16S rRNA transcript compared to the corresponding 60-nt synthetic DNA target (compare data in Figure 1A with that in Figure 2A). We hypothesize that the single-stranded overhanging segment of the target extends towards the electrode's surface and potentially disrupts the biosensor's

functionality. This disruption might occur through either binding to the electrode and creating a barrier that obstructs the Red/Ox label interaction, or by interfering with the adjacent probe-target binding, ultimately resulting in a reduction of the electrochemical signal. Surprisingly, the 5WJ biosensor produced an astonishingly high signal in the presence of 16S rRNA transcript (S/B ~25) unlike the hairpin probe,[42, 43] or X and 5S-X biosensors (S/B ~5 and 8, respectively) (Figure 2A).

DNA nanostructures have been reported to facilitate nucleic acid analysis. For example, localizing a probe as a part of a well-defined uniform DNA tetrahedron-structure on electrode surfaces enabled control of both the probe's density and orientation, thus increasing the probe-target interaction efficiency.[9-11] In the case of the 5WJ biosensor, it is possible that upon the target's binding, the construct acquires a conformation, in which the MB label points toward the electrode. This conformation thus may be optimal for producing a high signal. At the same time, the fragments of the target that are not associated with the biosensor's components remain away from the electrode surface, as shown in Scheme 1D and S1, without disturbing the electron transfer. Further experiments are needed to confirm this hypothesis, as well as to facilitate the kinetics of the 5WJ formation.

All three biosensors studied in this work can be designed to tightly bind the analyzed nucleic acid sequence by one arm and, at the same time, selectively interrogate the target by another. For example, the f-strand of the 5WJ biosensor contained a 21-nt sequence complementary to a fragment of 16S rRNA (Scheme S1). It, therefore, enabled tight, but not very selective binding to the target (under experimental conditions). However, the full signal-producing 5WJ complex is formed only when m-stand, with an 8-nt target-binding arm, binds 16S rRNA with high selectivity. Indeed, the probe reliably distinguished the fully matched from a two-base pair mismatched target (Figure 1A). Similar design with the X biosensors enabled differentiation of single-base mutations with just a background-level signal triggered by a mismatched target,[29] a performance that cannot be achieved even by the most recent developments in the thermodynamics-based approaches.[44]

Several recent studies have demonstrated impressive LOD, ranging from 2.8 to 10 fM, and even reaching up to 10 CFU/mL. These achievements were realized by utilizing DNA linear probes with biotin-labeled reporters,[45] microfluidic chip devices,[46] or nanocomposites based on molybdenum disulfide,[47] with detection times spanning between 80 minutes to 4 hours. While these outcomes are noteworthy, there is room for improvement by employing stem-loop probes. Comparative studies with linear probes have shown that stem-loop probes exhibit superior performance.[48] In particular, the use of multicomponent probe systems such as X, 5S-X, or 5WJ designs, integrating standardized probes like UDH, has proven effective. These structures allow a single probe to be employed for the detection of multiple systems. Moreover, they offer the advantage of probe reusability with minimal signal loss.

Conclusions

In conclusion, we adopted a nucleic acid 5WJ structure for electrochemical analysis of nucleic acids. The unique property of the 5WJ-forming biosensor is to detect a long and structured RNA target with high signal-to-background ratio (as demonstrated with *E. coli* 16S rRNA transcript). 5WJ biosensor provided a measurable response to the presence of the target in the total bacterial RNA preparation with and LOD of 0.44nM. The 5WJ biosensor demonstrated high selectivity at room temperature. Moreover, both the electrode-attached strand (UDH) and Red/Ox marker-labelled strand (MB-probe) were universal: they can be optimized once and then used for the analysis of potentially any nucleic acids. We believe this multipurpose biosensor is a development that will facilitate the application of DNA nanotechnology in medical diagnostics.

Author Contributions

Marcos V. Foguel – data curation, formal analysis, investigation, methodology, validation, visualization, writing – original draft, review and editing. Victor Zamora – investigation, methodology, writing – review and editing. Julio Ojeda – formal analysis, validation, writing-review and editing. Mark Reed – investigation, methodology, writing – review and editing. Alexander Bennett – investigation, methodology, writing – review and editing. Percy Calvo-Marzal – conceptualization, methodology, project administration, supervision, validation, writing – review and editing. Yulia V. Gerasimova – conceptualization, methodology, project administration, supervision, validation, writing – review and editing. Dmitry Kolpashchikov – conceptualization, methodology, project administration, supervision, validation, writing – review and editing. Karin Y. Chumbimuni-Torres – conceptualization, funding acquisition, methodology, project administration, resources, supervision, validation, writing – review and editing.

Conflicts of interest

There are no conflicts to declare.

Acknowledgements

The authors acknowledge NSF-CBET grant number #1706802 and Florida Health Department grant #7ZK05.

References

1. N. C. Seeman and H. F. Sleiman, *Nature Reviews Materials*, 2017, **3**, 17068.
2. A. C. Hill and J. Hall, *Materials Chemistry Frontiers*, 2020, **4**, 1074-1088.
3. H. Ramezani and H. Dietz, *Nat Rev Genet*, 2020, **21**, 5-26.
4. Q. Zhang, Q. Jiang, N. Li, L. Dai, Q. Liu, L. Song, J. Wang, Y. Li, J. Tian, B. Ding and Y. Du, *ACS Nano*, 2014, **8**, 6633-6643.
5. E. Tasciotti, *Nat Biotechnol*, 2018, **36**, 234-235.
6. A. Udomprasert and T. Kangsamaksin, *Cancer Sci*, 2017, **108**, 1535-1543.

7. H. K. Subramanian, B. Chakraborty, R. Sha and N. C. Seeman, *Nano Lett*, 2011, **11**, 910-913.
8. T. Funck, F. Nicoli, A. Kuzyk and T. Liedl, *Angew Chem Int Ed Engl*, 2018, **57**, 13495-13498.
9. A. Abi, M. Lin, H. Pei, C. Fan, E. E. Ferapontova and X. Zuo, *ACS Appl Mater Interfaces*, 2014, **6**, 8928-8931.
10. F. Xu, H. Dong, Y. Cao, H. Lu, X. Meng, W. Dai, X. Zhang, K. A. Al-Ghanim and S. Mahboob, *ACS Appl Mater Interfaces*, 2016, **8**, 33499-33505.
11. J. Lu, J. Wang, X. Hu, E. Gyimah, S. Yakubu, K. Wang, X. Wu and Z. Zhang, *Anal Chem*, 2019, **91**, 7353-7359.
12. D. M. Kolpashchikov, *Acc Chem Res*, 2019, **52**, 1949-1956.
13. S. Kogikoski, W. J. Paschoalino, L. Cantelli, W. Silva and L. T. Kubota, *TrAC Trends in Analytical Chemistry*, 2019, **118**, 597-605.
14. T. G. Drummond, M. G. Hill and J. K. Barton, *Nat Biotechnol*, 2003, **21**, 1192-1199.
15. S. Campuzano, M. Pedrero and J. M. Pingarron, *Anal Bioanal Chem*, 2014, **406**, 27-33.
16. M. Labib and M. V. Berezovski, *Biosens Bioelectron*, 2015, **68**, 83-94.
17. M. Labib, E. H. Sargent and S. O. Kelley, *Chem Rev*, 2016, **116**, 9001-9090.
18. E. E. Ferapontova, *Annu Rev Anal Chem (Palo Alto Calif)*, 2018, **11**, 197-218.
19. P. Gillespie, S. Ladame and D. O'Hare, *Analyst*, 2018, **144**, 114-129.
20. M. K. Masud, M. Umer, M. S. A. Hossain, Y. Yamauchi, N. T. Nguyen and M. J. A. Shiddiky, *Trends Biochem Sci*, 2019, **44**, 433-452.
21. Z. Shabaninejad, F. Yousefi, A. Movahedpour, Y. Ghasemi, S. Dokanehiifard, S. Rezaei, R. Aryan, A. Savardashtaki and H. Mirzaei, *Anal Biochem*, 2019, **581**, 113349.
22. P. Yanez-Sedeno, L. Agui, S. Campuzano and J. M. Pingarron, *Biosensors (Basel)*, 2019, **9**, 127.
23. D. X. Wang, J. Wang, Y. X. Wang, Y. C. Du, Y. Huang, A. N. Tang, Y. X. Cui and D. M. Kong, *Chem Sci*, 2021, **12**, 7602-7622.
24. Y. Xiao, R. Y. Lai and K. W. Plaxco, *Nat Protoc*, 2007, **2**, 2875-2880.
25. M. Labib, S. M. Ghobadloo, N. Khan, D. M. Kolpashchikov and M. V. Berezovski, *Anal Chem*, 2013, **85**, 9422-9427.
26. D. M. Mills, P. Calvo-Marzal, J. M. Pinzon, S. Armas, D. M. Kolpashchikov and K. Y. Chumbimuni-Torres, *Electroanalysis*, 2017, **29**, 873-879.
27. D. M. Kolpashchikov, *Chem Rev*, 2010, **110**, 4709-4723.
28. M. Stancescu, T. A. Fedotova, J. Hooyberghs, A. Balaeff and D. M. Kolpashchikov, *J Am Chem Soc*, 2016, **138**, 13465-13468.
29. S.-C. Sun, H.-Y. Dou, M.-C. Chuang and D. M. Kolpashchikov, *Sensors and Actuators B: Chemical*, 2019, **287**, 569-575.
30. D. M. Mills, M. V. Foguel, C. P. Martin, T. T. Trieu, O. Kamar, P. Calvo-Marzal, D. M. Kolpashchikov and K. Y. Chumbimuni-Torres, *Sensors and Actuators B: Chemical*, 2019, **293**, 11-15.
31. H. Ravan, *TrAC Trends in Analytical Chemistry*, 2015, **65**, 97-106.
32. Y. L. Wang, J. E. Mueller, B. Kemper and N. C. Seeman, *Biochemistry*, 1991, **30**, 5667-5674.
33. J. L. Kadrmas, A. J. Ravin and N. B. Leontis, *Nucleic Acids Res*, 1995, **23**, 2212-2222.
34. R. F. Carvalhal, R. Sanches Freire and L. T. Kubota, *Electroanalysis*, 2005, **17**, 1251-1259.
35. S. Trasatti and O. A. Petrii, *Journal of Electroanalytical Chemistry*, 1992, **327**, 353-376.
36. N. Bhatt, P. J. Huang, N. Dave and J. Liu, *Langmuir*, 2011, **27**, 6132-6137.
37. C. A. Lynch, 3rd, M. V. Foguel, A. J. Reed, A. M. Balcarcel, P. Calvo-Marzal, Y. V. Gerasimova and K. Y. Chumbimuni-Torres, *Anal Chem*, 2019, **91**, 13458-13464.
38. J. S. Johnson, D. J. Spakowicz, B. Y. Hong, L. M. Petersen, P. Demkowicz, L. Chen, S. R. Leopold, B. M. Hanson, H. O. Agresta, M. Gerstein, E. Sodergren and G. M. Weinstock, *Nat Commun*, 2019, **10**, 5029.
39. A. Akram, M. Maley, I. Gosbell, T. Nguyen and R. Chavada, *Int J Infect Dis*, 2017, **57**, 144-149.
40. A. Albihn, E. Eriksson, C. Wallen and A. Aspan, *Acta Vet Scand*, 2003, **44**, 43-52.
41. M. Fessler, B. Gummesson, G. Charbon, S. L. Svenningsen and M. A. Sorensen, *Mol Microbiol*, 2020, **113**, 951-963.
42. B. Bockisch, T. Grunwald, E. Spillner and R. Bredehorst, *Nucleic Acids Res*, 2005, **33**, e101.
43. C. Liu, G. M. Zeng, L. Tang, Y. Zhang, Y. P. Li, Y. Y. Liu, Z. Li, M. S. Wu and J. Luo, *Enzyme Microb Technol*, 2011, **49**, 266-271.
44. F. Can, H. E. Okten, T. Ergon-Can, P. Ergenekon, M. Ozkan and E. Erhan, *Bioelectrochemistry*, 2020, **135**, 107553.
45. Q. Wang, Y. Wen, Y. Li, W. Liang, W. Li, Y. Li, J. Wu, H. Zhu, K. Zhao, J. Zhang, N. Jia, W. Deng and G. Liu, *Anal Chem*, 2019, **91**, 9277-9283.
46. H. Ghorbanpoor, A. N. Dizaji, I. Akcakoca, E. O. Blair, Y. Ozturk, P. Hoskisson, T. Kocagoz, H. Avci, D. K. Corrigan and F. D. Guzel, *Sensors and Actuators A: Physical*, 2022, **339**.
47. L. Yuwen, X. Li, L. Wu, Y. Luo and S. Su, *Analyst*, 2023, **148**, 6292-6296.
48. R. Y. Lai, B. Walker, K. Stormberg, A. J. Zaitouna and W. Yang, *Methods*, 2013, **64**, 267-275.